Journal of Environmental Chemical Engineering 13 (2025) 116165

Contents lists available at ScienceDirect

Journal of Environmental Chemical Engineering

journal homepage: www.elsevier.com/locate/jece

Fostering the performance and stability of the high-rate activated sludge process: Biomass dynamics, oxygen consumption and clarifier operation

Joan Canals [a,b], Alba Cabrera-Codony [a,*], Oriol Carbó [a,b], Andrea Turolla [c], Sara García [b], Juan M. Lema [d], Hèctor Monclús [a]

[a] LEQUIA, Institute of the Environment, Universitat de Girona, C. Maria Aurèlia Capmany 69, Girona 17003, Spain
[b] GS Inima Environment, S.A. C/ Gobelas 41 1ª, Madrid 28023, Spain
[c] Politecnico di Milano, Department of Civil and Environmental Engineering (DICA), Piazza Leonardo da Vinci 32, Milano 20133, Italy
[d] CRETUS, Department of Chemical Engineering, University of Santiago de Compostela, Santiago de Compostela 15782, Spain

ARTICLE INFO

Keywords:
High-rate activated sludge
COD harvesting
Oxygen uptake rate
Clarifier performance
Solid flux analysis
Settling characteristics

ABSTRACT

The optimization of performance and long-term stability of a demonstration-scale High-Rate Activated Sludge (HRAS) pilot plant for treating urban wastewater treatment (35 m^3 d^{-1}) was evaluated over 497 days. Maintaining the mixed liquor suspended solids (MLSS) concentration between 1800 and 2100 mg L^{-1} through waste sludge adjustment stabilizes the operation, preventing biomass washout and sludge bulking. Despite significant fluctuations in influent chemical oxygen demand (COD), ranging from 340 to 1580 mg L^{-1}, the system consistently achieved an organic removal ratio of 58 %, even under elevated loading conditions, with a low oxidation rate of only 6.9 % ± 3.6 %. Oxygen management was crucial for a high system's performance. The oxygen uptake rate (OUR) ranged from 31 to 54 mg_{O2} L^{-1} h^{-1}, and the specific oxygen consumption (SOC) averaged 0.9 kg_{O2} $kg_{CODrem^{-1}}$. The study highlighted the potential of using soluble COD SOC as an effective parameter for optimizing oxygen supply. The study also evaluated solids removal efficiency using clarifiers of different diameters. The influent suspended solids (SS) removal efficiency increased from 71 % in a 1.0 m diameter clarifier to 85 % in a 1.4 m. The HRAS efficiently acted as a filter for the SS influent's peak loads, buffering the load to the CAS process. A detailed sludge stratification analysis revealed a balanced biomass distribution between the reactor and clarifier, with 50 % of the total biomass retained in the clarifier. Solids flux analysis confirmed that the system was not limited by solids loading but rather by hydraulic loading, with potential improvements achievable through optimization of the overflow rate (OFR).

1. Introduction

Integrating HRAS systems into wastewater treatment, replacing the primary clarifiers (PC), represents a shift towards enhancing operational efficiency, minimizing environmental impact, and fostering resource recovery [1,2]. While effective, traditional wastewater treatment plants, based on conventional activated sludge (CAS) processes, often need to improve in addressing the growing environmental challenges. HRAS, as a combination of physical and biochemical separation processes, aim to optimize energy consumption while reducing the COD oxidation, i.e., ensuring the most significant COD harvesting to send to anaerobic digestion [3–5].

Recent studies have highlighted the role of different HRAS configurations in optimizing performance across varying influent conditions. Rahman et al. [6] categorized three main HRAS configurations: HRAS (A-Stage) for treating high-strength influents such as raw municipal wastewater, High-Rate Contact Stabilization (CS) for influents with lower organic matter concentrations, such as those from chemically enhanced primary treatment (CEPT), and HRAS Sludge Batch Reactor (SBR) for treatment systems operating in colder climates and under highly variable loads. Additionally, Tirkey et al. [7] explored an anoxic HRAS configuration that enhances denitrification and carbon recovery through B-Stage effluent recirculation. These configurations highlight the adaptability of HRAS systems to diverse wastewater treatment scenarios and the potential for further optimization [8].

To explore the HRAS performance, it is necessary to differentiate the removal mechanisms of COD fractions [9]. Soluble COD (sCOD) is mainly removed through biological processes such as microbial

* Corresponding author.
E-mail address: alba.cabrera@udg.edu (A. Cabrera-Codony).

https://doi.org/10.1016/j.jece.2025.116165
Received 20 December 2024; Received in revised form 7 March 2025; Accepted 11 March 2025
Available online 15 March 2025

metabolism or cell storage. In contrast, particulate (pCOD) and colloidal COD (cCOD) are mostly captured through physical mechanisms like bioadsorption, bioflocculation and bioaccumulation [10]. Suspended solids (SS) are separated through sedimentation [11,12]. Achieving high biomass concentration and rapid sedimentation rates is essential for efficient COD harvesting within a compact design [7,13].

Solids Retention Time (SRT) is one of the most critical parameters influencing the balance between biosorption, flocculation, and microbial metabolism [6]. Early studies on A-stage HRAS systems operated at SRTs below 2 days [14,15], while more recent investigations have refined this range further to enhance carbon capture while minimizing oxidation [6,9,16]. At SRT below 0.5 days biosorption dominates, with rapid enmeshment of pCOD and cCOD into sludge flocs, which are removed with the excess sludge, and a fraction of sCOD assimilated via intracellular storage and oxidation [16], leaving sufficient readily biodegradable carbon for denitrification in the B-stage [17]. As SRT increases from 0.5 to 1.0 days hydrolysis starts playing a greater role in COD removal, gradually shifting the process from biosorption to biological degradation. However, operating at higher SRTs (>1.5 days) increases COD oxidation, reducing its carbon redirection potential [16].

Under low SRT conditions, sCOD removal is more influenced by influent heterotrophic biomass than by new biomass growth within the reactor [16,18,19]. This suggests that mixed liquor suspended solids (MLSS) should be optimized alongside SRT to maintain sludge settleability. Early research observed that HRAS primarily supports the growth of the rapid-growing bacteria (AHO), unlike CAS systems, which host a diverse microbial community [18,20–22]. Due to the low SRT, HRAS retains only the AHO organisms capable of utilizing rapidly degradable substrates such as volatile fatty acids (VFA) and monomers, enhancing carbon capture while minimizing cell lysis and endogenous respiration, which in turn minimizes oxygen consumption [20–23] Also, the young, fast-growing sludge produced at SRT < 0.3 days is more easily digested in anaerobic digestion, contributing to higher methane yields [24]. However, extremely low SRTs (<0.1 days) may reduce sludge settleability, impacting process stability [23,24].

Hydraulic retention time (HRT) plays a crucial role in determining whether the HRAS process favours biosorption or oxidation [25,26]. Studies have established that HRT should remain below 60 min to minimize COD mineralization [27]. Shorter HRTs (~30 min), as used in [1,23,28], are associated with enhanced bioadsorption, allowing rapid COD capture before oxidation occurs. Increasing HRT beyond 60 min shifts the process towards bio-oxidation, reducing the COD fraction available for anaerobic digestion [14].

MLSS concentration is crucial for retaining active biomass and enhancing carbon adsorption. Studies show that operating MLSS up to 3000 mg/L supports bioflocculation and enhances COD capture without significantly impacting oxygen transfer efficiency [16,19]. Zhao et al. [29] studied MLSS from 0.5 g/L to 6 g/L, observing sCOD removal up to 30 %, indicating that MLSS is particularly important for sCOD capture.

Furthermore, a key point of the HRAS system operation lies in oxygen management, which necessitates precise control to balance the dichotomy between microbial respiration needs and energy efficiency [30]. In the early stages of this technology development, Böhnke [18] suggested that HRAS could be operated near zero dissolved oxygen (DO) in facultative mode, with the oxygen supplied solely by grit and grease removal processes in the preceding stages. Later studies by [16,31,32] worked successfully with DO concentrations in HRAS reactors from 0.1 to 2 $mgO_2\ L^{-1}$. Most recently, Hauduc et al. [28] showed a positive correlation between oxygen demand and sCOD removal, emphasising the need for oxygen supply system control optimization.

Thus, one of the main questions raised on the process design is: what is the most effective method for controlling the oxygen supplied while minimizing COD oxidation? Different control approaches include maintaining constant DO in the reactor, setting an hourly oxygen supply pattern or real-time control based on sCOD measurements [12]. In this context, we identified the sCOD oxidation as the most challenging parameter to control and the specific oxygen consumption (SOC) as an indicator of the system energy efficiency, reflecting the oxygen demand for organic matter removal, and will examine it for insights into the optimization of aeration strategies.

Again, sludge settleability is key in clarifier performance and overall efficiency in HRAS systems. The effectiveness of solid-liquid separation in clarifiers is determined by sludge physical properties, specifically the Sludge Volume Index (SVI) and Zone Settling Velocity (ZSV), and the hydrodynamics in the settler, overflow rate (OFR) and solids loading rate (SLR) [33–38]. Distinct from traditional primary (PC) and secondary (SC) clarifiers, the HRAS clarifiers handle a unique mix and quantity of SS, influencing settling mechanisms. HRAS clarifiers receive a blend of HRAS biomass and incoming SS ranging from 2300 ± 400 mg L^{-1}. In contrast, PCs directly process influent wastewater SS, typically at 100–300 mg L^{-1}, while SCs deal with biological sludges at concentrations around 2000 to 4000 mg L^{-1}. In addition, a significant operational difference is the target effluent SS concentration: HRAS clarifiers aim for optimal COD harvesting with minimal energy use, similar to PCs, whereas SCs must comply with stringent SS regulatory limits of 10–20 mg L^{-1}.

In detail, the design of PCs is based on discrete particle and flocculent settling analyses, and its efficiency depends on influent wastewater characteristics, particularly the SS concentration and the proportion of settleable solids, as well as operational parameters like HRT and OFR [39]. Otherwise, SCs and HRAS clarifiers present multiple settling regimes due to the high SS concentrations and flocculated state. These include discrete flocculent settling at the surface, hindered settling within the incoming sludge mass, and compressive settling within the sludge blanket at the bottom [39]. HRAS clarifier, distinguished by a lower SVI, contrasts with SC, where SLR is a critical parameter, and positions HRAS as a system capable of extensive SS and COD removal through the adsorption of non-settleable and colloidal material and the sCOD storage not seen in PC.

In this study, we provide a holistic approach towards HRAS system optimization. Over 497 operation days in a demonstration pilot plant of 35 $m^3\ day^{-1}$ capacity, we comprehensively evaluated the performance and stability over different operation conditions, aiming to gain insights into its capacity for removing COD, BOD_5, and SS under varying organic loading rates. This long-term evaluation allows us to explore the system's ability to buffer peak loads while maintaining stable treatment performance.

The research focuses on optimising operational parameters such as MLSS concentration, SRT, and oxygen supply, which are critical to minimize COD oxidation. Special attention is given to oxygen consumption, where the dynamics of SOC and OUR are analysed to inform aeration strategies to improve energy efficiency. Additionally, the study examines the settling characteristics of HRAS biomass and the effectiveness of solid-liquid separation in the clarifier using two different clarifiers, considering factors such as SVI and ZSV. The research seeks to understand how influent variability and clarifier operational parameters affect sludge settleability and system performance. Ultimately, this work aims to optimize the HRAS process, offering insights into its operational sustainability and treatment efficacy.

2. Materials and methods

2.1. Pilot plant and operation conditions

A demonstration-scale pilot plant, depicted in Supplementary Information (Fig. S1), was constructed and operated using municipal wastewater sourced from the wastewater treatment plant (WWTP) in Montornès del Vallès (Barcelona, Northeast Spain). This facility serves 95,000 equivalent inhabitants, with significant load fluctuations due to industrial activities (30–40 %). The pilot plant was operated for 497 days treating raw wastewater after grit and scum removal with a daily influent flow rate ranging from 21 to 35 $m^3\ day^{-1}$.

2.1.1. Reactors

The pilot plant setup included two in-series biological reactors (R1 and R2), each with a volume of 0.8 m^3 and a water depth of 3 m. The combined HRT of the reactors (R1 + R2) ranged between 0.6 and 1.6 h, while the SRT was maintained at 0.2 ± 0.05 days to minimize sCOD oxidation. The pilot plant presented a reduced surface-water depth in the reactor compared to conventional full-scale systems, which may hamper flocculation efficiency. R1, positioned upstream of the aerobic R2 reactor, was operated only during the first 350 days to assess its potential to enhance flocculation. Thus, in anoxic R1 reactor, coarse bubbles were used solely to keep the biomass in suspension without DO control. The oxygen supply in R2 was controlled through a DO sensor and an automated PID-controlled opening air valve (OAV). Fine bubbles were used for aeration and mixing, maintaining a DO set point between 0.5 and 1 mg L^{-1}. The reactor temperature ranged between 18.5 and 26.3 °C without any correction.

2.1.2. Clarifiers

Two clarifiers of different diameters - 1.0 m (used from days 1–320) and 1.4 m (used from days 321–497) - were operated to investigate the effect of SLR and OFR on the performance of solid separation without altering the reactor HRT, where:

$$OFR = \frac{Q_{in}}{\text{Clarifier surface}} \quad (1)$$

$$SLR = \frac{(Q_{in} + Q_r)\cdot MLSS}{\text{Clarifier surface}} \quad (2)$$

Where MLSS is the solids concentration in the R2 reactor, Q_{in} is the influent flowrate and Q_r is the recirculation flowrate.

The 1.0 m clarifier was chosen to reflect PC conditions with an OFR of ~1.6 m h^{-1}, within the reported PC design range (1.2–2.0 m h^{-1}). The 1.4 m clarifier operated at a lower OFR (~0.8 m h^{-1}), similar to SC in CAS systems (0.66–1.6 m h^{-1}). This setup enabled a direct assessment of clarifier sizing impacts on sludge stratification and effluent quality under the same influent conditions.

The sludge volume index (SVI) was measured using a 1 L graduated cylinder to record the height of the sludge at 5-min intervals during the settling process. SVI_{30} represents the sludge blanket at 30 min, divided by the MLSS concentration. The clarifiers had five sampling points at various heights (Fig. S2) to analyse SS concentration. Up to operation day 85, waste was collected from Reactor R2, while from day 86 onward, waste was diverted from the clarifier. The recirculation flow rate was maintained at a minimum of 60 % of the influent flow rate. Waste activated sludge was pumped at a rate of 0.5 m^3 h^{-1} using a helicoidal pump, which operated on an ON/OFF switching mechanism controlled by the MLSS set point to ensure a constant and low MLSS concentration in the reactor, preventing biomass washout, minimizing the solid load in the settling tank, and avoiding the formation of poorly settling sludge.

2.2. Sampling and analysis

SS concentration was continuously monitored by online sensors positioned in the reactor, and influent, waste activated sludge, return activated sludge and effluent flows. To quantify the effect of incoming SS in the HRAS process, we introduced the SER as the ratio between reactor biomass inventory and daily solids feed, according to:

$$SER = \frac{V\cdot MLSS}{Q_{in}\cdot SS_{in}} \quad (3)$$

Where V is the reactor R2 volume and SS_{in} is the suspended solids concentration in the influent.

Automatic samplers were used to collect and keep refrigerated integrated samples from both the influent and the effluent streams. The analysis included BOD_5 and COD fractions, where pCOD is the difference between total COD and COD filtered through a 1.5 μm filter; sCOD was determined by flocculation with $ZnSO_4$ and filtration through 0.45 μm filter; cCOD is difference between pCOD and sCOD.

The COD removed is the difference between the influent and the effluent COD, and it includes both the wasted and the oxidized COD. Thus, COD oxidation was evaluated by the mass balance considering the removed and the wasted COD.

The organic loading ratio (OLR) is the ratio between the influent COD load and the MLSS inventory in R2. In contrast, the organic removal ratio (ORR) is the corresponding COD removal ratio in the water line.

$$OLR = \frac{Q_{in}\cdot COD_{in}}{V\cdot MLSS} \quad (4)$$

$$ORR = \frac{Q_{in}\cdot COD_{in} - Q_{out}\cdot COD_{out}}{V\cdot MLSS} \quad (5)$$

2.3. Oxygen control

Continuous monitoring of DO concentration and OAV position (as an opening percentage, %OAV) was conducted using online sensors recording data every 5 s and calculating 1-min averages. The DO sensor was installed at half the height of the water column. A minimum 32 % OAV position was fixed to prevent biomass settling in the reactors.

The oxygen consumption in the R2 reactor was accurately evaluated by continuous calculation of the oxygen uptake rate (OUR). This involved first establishing the mass coefficient (k_La) in clean water as a function of the %OAV. R2 reactor was equipped with a fine bubble diffuser (SULCER 9), providing a superficial diffuser density of 18 %. The reactor was initially filled with clean water, from which oxygen was displaced with nitrogen to reach an initial oxygen concentration close to zero. We assumed that the total volume (V_T) (water + bubbles) was equal to the volume of water (V_L) [40]. Adjusting the OAV position, DO was monitored at a water depth of 1.5 m. k_La was obtained as:

$$k_La_T = \ln\frac{DO_{sat(T)} - DO_T(t_0)}{DO_{sat(T)} - DO_T(t)}\cdot\frac{1}{t - t_0} \quad (6)$$

Where k_La is the oxygen mass transfer coefficient [h^{-1}] at the working temperature (T), $DO_{sat(T)}$ is the DO saturation at T, $DO_T(t)$ is the DO in the reactor [mgO_2 L^{-1}] at time t and $DO_T(t_0)$ is the DO at the initial time t_0. The effect of temperature on oxygen transfer was established by using Eq. (7), where the coefficient Θ for fine bubble diffuser was set equal to 1.024 [39]:

$$k_La_T = k_La_{20°C}\cdot\theta^{T-20} \quad (7)$$

OUR [$mgO_2\cdot L^{-1}\cdot h^{-1}$] represents the rate at which the oxygen is consumed per unit of time and reactor volume. k_La value was used to calculate OUR according to the DO mass balance in the liquid phase:

$$OUR_t = \alpha\cdot k_La_T\cdot[\beta\cdot DO_{sat(T)} - DO_{(T)}(t)] - \frac{dDO}{dt} \quad (8)$$

Where α is $\frac{k_La_{(wastewater)}}{k_La_{(cleanwater)}}$ and ß is $\frac{DO_{sat(wastewater)}}{DO_{sat(cleanwater)}}$. α-factor of 0.48 and β-factor of 0.98 were considered according to [41]. No fouling factors were considered.

The specific oxygen consumption for COD (SOC_{COD}), sCOD ($SOC_{s\text{-}COD}$) and BOD_5 (SOC_{BOD5}) relates the OUR with the organic matter removal as:

$$SOC_{COD} = \frac{OUR\cdot V}{Q_{in}\cdot COD_{in} - Q_{out}\cdot COD_{out}} \quad (9)$$

$$SOC_{sCOD} = \frac{OUR\cdot V}{Q_{in}\cdot sCOD_{in} - \quad Q_{out}\cdot sCOD_{out}} \quad (10)$$

$$SOC_{BOD5} = \frac{OUR \cdot V}{Q_{in} \cdot BOD_{5in} - Q_{out} \cdot BOD_{5out}} \quad (11)$$

2.4. Solids dynamics

Batch settling tests were conducted on sludge samples diluted to different initial MLSS concentrations to determine Zone Settling Velocity (ZSV) [42]. The exponential decaying function that matches the ZSV and the initial solids concentration is the Vesilind model [43]:

$$V_{hs}(X) = V_0 \cdot e^{-r_h \cdot X} \quad (12)$$

Where $V_{hs}(X)$ is the ZSV of the sludge [m h^{-1}] at X solids concentration [g L^{-1}], V_0 is the calibration parameter corresponding to the maximum settling velocity [m h^{-1}], and r_h is the calibration parameter corresponding to the clarification zone [L·g^{-1}]. A solid flux model with five layers has been applied to understand further and validate the observed SS stratification in the clarifier. Each zone in the clarifier was described by the differential equations provided in the Supplementary Information (Equation S1-S6) based on the model by Takacs et al. [44].

The total solids flux (SF_t) in the clarifier is determined by combining the solids flux due to gravity (SF_g) and the solids flux resulting from bulk movement (SF_u).

$$SF_t = SF_g + SF_u \quad (13)$$

$$SF_g = V_g \cdot X \quad (14)$$

$$SF_u = V_b \cdot X \quad (15)$$

where V_b is the bulk downward velocity [m h^{-1}], and Vg is the gravity velocity calculated according to [44]:

$$V_g(X) = V_0 \cdot e^{-r_h \cdot X} - V_0 \cdot e^{-r_p \cdot X} \quad (16)$$

where r_p is the settling parameter for low solid concentration.

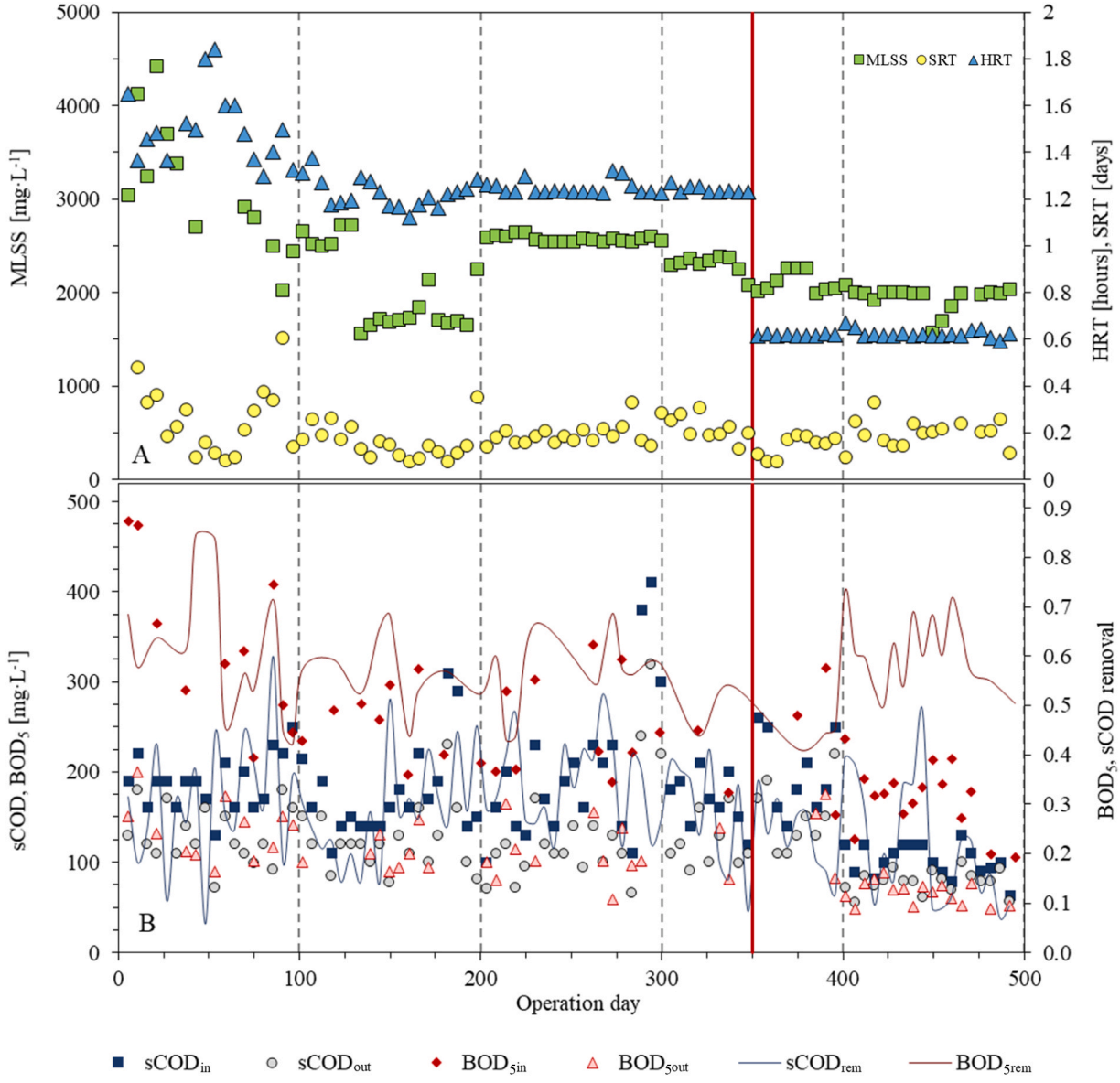

Fig. 1. Daily monitoring of A) MLSS, SRT and HRT in the HRAS reactor and B) sCOD and BOD_5 concentrations at the influent and effluent, and their removal efficiency. The vertical solid red line indicates the transition from operating both reactors (R1 +R2) to operating R2 alone.

3. Results and discussion

3.1. Process performance and stability

This study provides a comprehensive analysis of the performance optimization and long-term stability of the HRAS process over 497 days. Ensuring stable operation requires balancing multiple factors, with MLSS concentration being one of the most critical indicators of reactor stability to optimize biomass retention, flocculation efficiency, and effluent quality. Exceeding 2500 mg L^{-1} led to SS leakage, while dropping below 1500 mg L^{-1} compromises flocculation. We evaluated the MLSS set point as a system control strategy, setting it between 1700 and 2500 mg L^{-1} [17].

3.1.1. MLSS control strategy

The pilot plant system dynamically adjusted the waste sludge flow rate to keep the MLSS within the target range. Initially, sludge was wasted from the reactor, causing fluctuations in MLSS levels, hampering the system stability (Fig. 1). On operation day 86, the wasting point was shifted to the clarifier return line, hich improved process stability by allowing the system to adapt to influent variations while maintaining a stable microbial population and sludge properties.

After this modification, MLSS remained within the working range, with stabilized values at 1700 mg L^{-1} (days 135–200), 2500 mg L^{-1} (days 200–300), 2200 mg L^{-1} (days 300–380), and 2000 mg L^{-1} (days 380–500). The reduction of MLSS within this range slightly reduced the sCOD removal efficiency (Fig. 1B) as indicated in previous studies [9]

The low MLSS level were sufficient to prevent biomass washout, settling tank overload, and to the formation of poor settling sludge or pinpoint flocs [45,46]. The system dynamically adjusted the waste sludge flow rate to keep MLSS within the target range, preventing excessive biomass accumulation and ensuring consistent oxygen demand, enhanced biosorption, and stable organic matter removal even under variable influent conditions.

3.1.2. SRT and carbon redirection

Using MLSS setpoint as a system control, the SRT was maintained at 0.2 ± 0.05 days, facilitating efficient biosorption of organic material while minimizing excessive sludge production [21]. At such a low SRT, readily degradable COD was primarily removed through rapid assimilation and oxidation, while colloidal and particulate COD had limited time for hydrolysis [19]. This balance prevented excessive carbon loss through mineralization, aligning with the goal of carbon redirection [16].

Despite maintaining the low SRT, the system had to adapt to significant variations in influent COD, which ranged from 340 to 1580 mg L^{-1}, with sCOD varying between 65 and 740 mg L^{-1} and BOD_5 concentrations between 105 and 495 mg L^{-1}. This resulted in an average COD OLR of 10.5 ± 3.5 kg_{COD} kg_{MLSS}^{-1} d^{-1} (Fig. 2), which exceeds the typical HRAS process range of 6.4 – 8.3 kg_{sCOD} kg_{MLSS}^{-1} d^{-1} indicated by [32,47]. Despite these elevated organic loading conditions, the system consistently achieved a COD ORR of 58 %, demonstrating the effectiveness of the process.

Similarly, the system handled a BOD_5 OLR of 4.1 ± 1.5 kg_{BOD5} kg_{MLSS}^{-1} d^{-1}, surpassing the reported range for the CAS process of 0.2–0.6 kg_{BOD5} kg_{MLSS}^{-1} d^{-1} [48], achieving a BOD_5 ORR of 54 %. Additionally, the pilot plant was operated at sCOD OLR of 2.9 ± 1.2 kg_{sCOD} kg_{MLSS}^{-1} d^{-1}, resulting in an average sCOD ORR of 34 %.

As expected, higher OLR values led to increased ORR and sludge generation. The system counteracted this effect by adjusting the waste sludge flow rate to maintain the MLSS set point. The precise of sludge control management prevented excessive biomass accumulation and reactor overload, ensuring consistent oxygen demand, and stable organic matter removal, even under variable influent conditions.

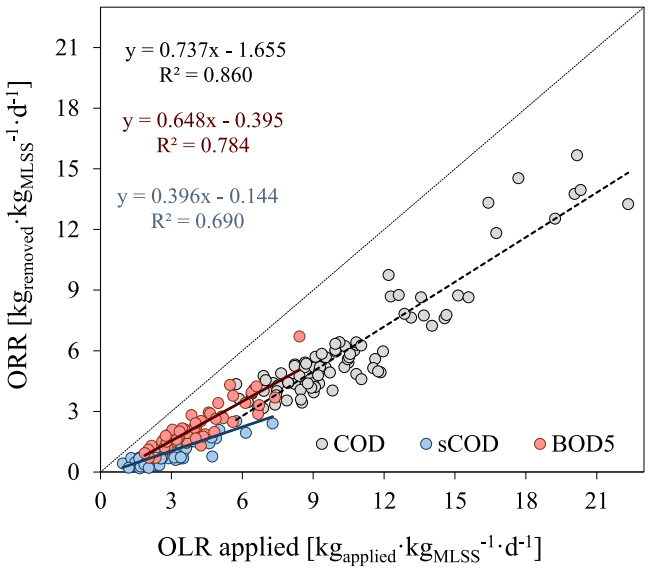

Fig. 2. Relation between OLR and ORR for COD, sCOD and BOD_5.

3.1.3. Reactor configuration

For the first 350 days, two reactors (R1 and R2, each 0.8 m^3) were operated in series, resulting in a combined HRT of approximately 1.2 h. After R1 was discontinued, R2 operated alone, reducing the total reactor volume and lowering the HRT to an average of 0.60 h (Fig. 1A). Despite this reduction, the controlled solids retention prevented biomass washout and maintained stable MLSS and SRT levels, ensuring sufficient biomass development and limiting excessive COD mineralization [25,26].

R1 was originally incorporated in the pilot plant to enhance flocculation, promoting the aggregation of suspended solids and microorganisms for improved particulate and soluble organic matter capture. For the first 350 days, R1 operated as an upstream unit with coarse bubble aeration to keep biomass suspended and prevent MLSS settling. After its decommissioning, R2 became the sole operational reactor. The removal of R1 did not result in significant changes in system performance, particularly regarding COD and BOD_5 removal, as no noticeable variations were observed before and after its removal (Fig. 1). This suggests that R1's flocculation role was not critical for organic matter removal in the HRAS system.

The stability of sCOD removal after R1's decommissioning confirms that R2 alone was sufficient for biosorption and sCOD removal. Since the HRAS system prioritizes rapid adsorption over full oxidation, R1's removal did not compromise its function.

3.2. Oxygen demand and control

3.2.1. Chemical oxygen demand

Throughout the operational period, the COD harvesting efficiency averaged 57 ± 9 % of the influent COD load, with average removal efficiency of 28 % for sCOD and 74 % for pCOD. Resulting from the mass balance calculation, the COD oxidation was of only 6.9 % ± 3.6 %, with an oxidation rate affected by the sCOD influent fraction: Increased influent sCOD over 200 mg L^{-1} resulted in the maximum oxidation of 14 % (Fig. S3 and Table S1 in Supporting Information). However, the oxidation values were notably lower than those reported by Miller et al. [19] (14 %) and Jimenez et al. [16] (22 %) and align with the optimal range of 6–7 % for energy savings indicated by Wett et al. [49].

To gain deeper insights into oxygen consumption, the COD fractions load was analysed over 6-h periods. Fig. 3A shows the distribution of the fractions using Day 274 to exemplify. I can be observed that the distribution was maintained throughout the day, with a notable reduction of

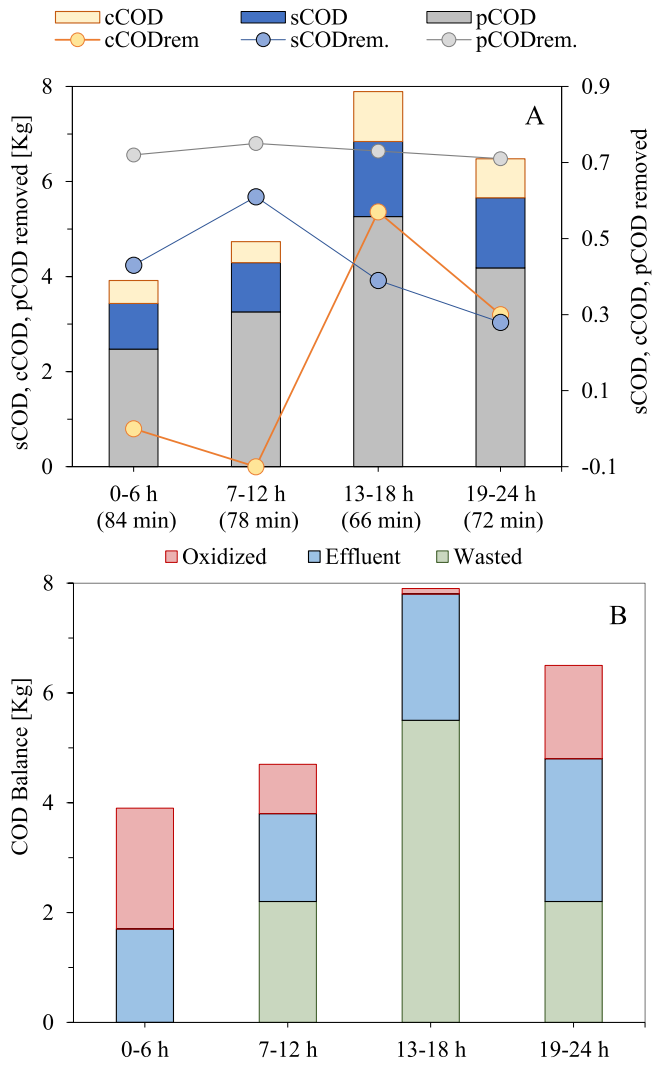

Fig. 3. Analysis of COD over six-hour periods in Day 274 detailing A) the COD fractions load (bars) and the corresponding removal efficiency for each fraction (dots), and B) the mass balance of the removed COD. Estimated HRT values in each period are reported in parentheses.

the total COD influent load during nocturnal hours compared to the 13–18 h period. The removal efficiency of pCOD, the fraction with the highest removal efficiency, remained constant throughout the day at around 74 %. In contrast, the removal efficiency of sCOD varied significantly, ranging from 28 % to 61 %. The removal of cCOD presents a highly variable range, even with a period (7–12 h) even displaying negative reduction, suggesting conversion of other fractions into colloidal forms.

The corresponding COD mass balance is presented in Fig. 3B. It can be observed that during the 0–6 h period, the oxidized COD was higher (56 %) than during the rest of the day: 21 % during the 19–24 h period, 19 % during the 7–12 h period, and only 1 % during the 13–18 h period, when the OUR presents its maximum values (Fig. S5). This suggests higher COD oxidation during nocturnal periods correlates with increased sCOD removal, highlighting the necessity of adjusting oxygen supply during these hours to minimize COD oxidation.

3.2.2. Oxygen uptake rate

To calculate the oxygen consumption as OUR at 20 °C, the k_La (Eq. (6)) was determined under different air flow rates by adjusting the % OAV; the results are presented in the Supplementary Information (Fig. S4) along with the corresponding logarithmic adjustment. Subsequently, the calculation of the oxygen consumption as OUR at 20 °C was performed for six days between operation days 430 and 480 when exclusively the reactor R2 was operated, facilitating the precise calculation of oxygen consumption (Table S2). Notably, the high surfactant content in the wastewater treated due to the absence of PC was addressed by applying a 0.48 α-factor to compensate for reduced oxygen transfer efficiency (Eq. 8) [49].

The obtained daily average OUR values ranged from 30 to 59 $mg_{O2}·L^{-1}·h^{-1}$. The reactor control successfully maintained constant DO levels at the set point by modulating the %OAV, as depicted in Fig. S5, where the 24-h monitoring of the DO online sensor, the %OAV and the calculation of the OUR is shown, demonstrating that the system effectively aligns the oxygen supply with the demand. However, in a scenario when the COD influent is particularly low, i.e. nocturnal hours, the system oxygen requirements are expected to diminish, and the imposition of a 32 % minimum on the OAV (to prevent biomass setting) could result in an excessive supply of oxygen. Given that the HRAS reactor operated at a low HRT, it had a low dilution rate, leading to high variability in OUR demands.

3.2.3. Specific oxygen consumption

After the OUR determination, the SOC at 20 °C was calculated using Eqs. 9–11 for the six days (see Table S2). It is important to notice that only the COD removed in the water line was considered, excluding the COD harvested for digestion. Fig. 4 presents the SOC values for COD, sCOD, and BOD_5 as a function of the removal efficiency.

The obtained SOC_{COD} values ranged from 0.08 to 0.18 kg_{O2} kg^{-1}_{CODrem}, aligned with those reported by [32] (0.13–0.21 kg_{O2} kg^{-1}_{CODrem}) and [50] (0.19 kg_{O2} kg^{-1}_{CODrem}), and lower than those reported by [16] (0.20–0.38 kg_{O2} kg^{-1}_{CODrem}). To gain deeper insights into SOC_{COD}, we examined the relationships between SOC_{COD} and COD removed. Fig. 4 reveals the relation between SOC_{COD} and the removal of COD: as removal increases, the SOC_{COD} slightly decreases, with a weak correlation coefficient, indicating that the SOC_{COD} is not a strong predictor of oxygen consumption dynamics.

The obtained SOC_{BOD5} values ranged from 0.23 to 0.453 kg_{O2} $kgs^{-1}_{BOD5rem}$. As depicted in Fig. 4, the relationship between SOC_{BOD5} and BOD_5 removal reveals a negative correlation, indicating that an increase in BOD_5 removal is associated with a reduction in the SOC_{BOD5} ratio. In this case, the higher correlation means that SOC_{BOD5} could be an effective metric for evaluating oxygen consumption efficiency.

Finally, the removal of sCOD presented a notable variation, ranging

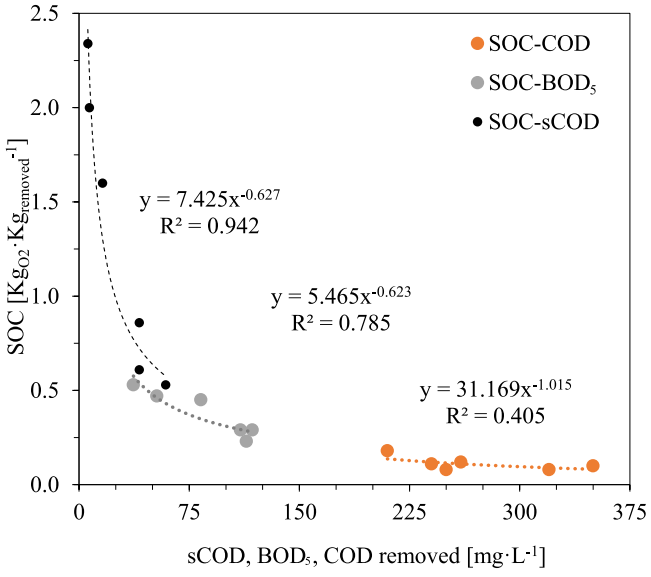

Fig. 4. SOC related to the removed COD, BOD_5 and sCOD.

from 7 % to 49 % depending on the day analysed and the influent concentration. Correspondingly, the SOC linked to sCOD removal (SOC_{sCOD}) exhibited a varied range from 0.53 to 2.34 kg_{O2} kgs^{-1}_{CODrem}. Days with very low influent sCOD ($\leq$100 mg L^{-1}) presented the highest SOC, likely due to the i) excessive air supply to maintain mixture conditions, ii) the presence of inorganic compounds (Fe^{2+}, H_2S) in the influent, and iii) low biodegradability, as indicated by BOD_5/COD falling below 0.22 (Table S2). However, Fig. 4 reveals that the SOC_{sCOD} is well correlated with the sCOD removal, suggesting that SOC_{sCOD} could serve as an effective parameter to control the oxygen supply aiming at the reduction of COD oxidation.

It is essential to notice that SOC concerning sCOD, COD and BOD_5 is not a stoichiometric measure but rather reflects the overall oxygen demand influenced by operational conditions and influent composition. The biodegradability of the influent, as indicated by the BOD_5/COD ratio, played a key role in determining oxygen consumption trends, as illustrated in Fig. S6, Supplementary Information. A higher BOD_5/COD ratio, indicative of more easily biodegradable wastewater, resulted in lower SOC, since easily biodegradable organic matter requires less oxygen for microbial metabolism.

Throughout the SOC analysis, the MLSS remained stable within the setpoint range, confirming that variations in SOC were driven by influent composition and removal efficiency rather than by changes in biomass concentration (Table S2). Given that the SRT was maintained at 0.2 $\pm$ 0.05 days, biological degradation of particulate and colloidal COD was limited, reinforcing biosorption as the dominant removal mechanism for these fractions. However, the oxygen demand associated with sCOD removal suggests that microbial oxidation still played a role in the degradation of the soluble fraction.

Two specific conditions were identified as contributors to increased COD oxidation. The first was on days a high fraction of sCOD in the influent, leading to higher oxygen demand due to direct microbial metabolism of soluble compounds. The second occurred during nocturnal periods when influent COD concentrations were low, resulting in excess oxygen availability that favoured oxidation over biosorption. While DO levels were maintained to prevent anoxic conditions, the fixed MLSS and SRT settings did not allow for real-time adjustments based on influent variations. This suggests that an oxygen supply strategy based on real-time sCOD measurements could optimize aeration efficiency, reduce unnecessary oxidation, and enhance carbon redirection in future operations [28].

3.3. HRAS biomass dynamics

3.3.1. Solids exchange ratio

A key distinction between HRAS and CAS systems lies in the role of influent SS in the biomass renewal, which is quantifiable through the SER. The SER reflects the biomass turnover rate, providing insights into how rapidly the system renew its microbial community. In the HRAS pilot plant, operating without PC, the SER was calculated (Eq. 3) as an average value of 0.15 $\pm$ 0.04 days, meaning that the influent SS can fully renew the 0.8 m^3 reactor biomass in 3.6 h.

For comparison, in a CAS system with PC, where HRT is 8 h and MLSS is 3 g L^{-1}, the MLSS, the SER typically exceeds four days. Additionally, the short SRT in the HRAS, at 0.1–0.3 days, further emphasizes the rapid biomass turnover, with complete renewal occurring approximately every 6 h. This analysis points out that the influent SS play a more significant role in biomass renewal than the SRT, suggesting that in HRAS systems, the influent SS properties primarily influence the settling characteristics rather than the growth of newly generated biomass, which underscores the importance of the solid exchange ratio (SER) as a key operational parameter.

To further assess the effects of rapid biomass turnover, MLSS samples were analysed for filamentous bacteria and protozoa (depicted in Fig. S7). Remarkably, over the 497-day operational period, no bulking phenomena were observed, even with DO concentration as low as 0.5 mg L^{-1}, aligning with the findings of Miller [19], who reported bulking only below 0.1 mg L^{-1} DO.

Contrary to the hypothesis by Böhnke et al. [18] that HRAS systems primarily support fast-growing bacteria, our findings reveal a more diverse microbial community, including both bacteria and protozoa. This microbial diversity can be attributed to the combination of influent wastewater composition and the return flows from side-stream solids treatment, which together form the HRAS influent. These results demonstrate that HRAS can sustain a diverse and resilient microbial community despite its high turnover rate, challenging the assumption that only CAS systems foster such complexity. Recent studies have further explored this microbial adaptability under HRAS conditions [51].

3.3.2. Sludge volume index

The SVI_{30}, the ratio between the volume of the solid after 30 min of settling and the MLSS concentration is a key indicator of sludge settleability in biological processes. The average SVI_{30} value of 55 $\pm$ 7 mL g^{-1}, as shown in Fig. 5A, contrasts with the typical CAS process values of 80–120 mL g^{-1} [48]. This lower SVI_{30} suggests faster sludge settling in HRAS compared to CAS. Previous studies [52–54] corroborate the observation of lower SVI values in HRAS, highlighting their beneficial effect on settleability.

However, measured SVI values at 5, 10, and 30-min intervals - 118, 87, and 56 mL g^{-1}, respectively exceeded those for granular or heavily flocculated sludges (70, 60, 55 mL g^{-1}) [55], indicating that HRAS sludge settles faster than CAS processes but slower than granular sludges, with an SVI_{10}/SVI_{30} ratio closer to one. Nonetheless, it is essential to acknowledge that while SVI serves as an influential qualitative gauge of settling tendencies, it does not offer quantitative insights into effluent quality [56]. Therefore, the effluent may still contain non-settleable solids that are not accounted for by the SVI measurement.

The favourable microbial composition and settling characteristics driven by influent SS suggest that incorporating PC is unnecessary. Avoiding the complexity and potential settleability reduction associated with primary clarifiers simplifies the treatment process, effectively allowing the HRAS system to handle influent loads without additional infrastructure.

3.4. Suspended solids removal

Focusing on the SS removal efficiency, Fig. 5B illustrates the daily evolution of the influent and effluent SS concentration and their removal efficiency for the two clarifiers evaluated in the pilot plant. The selection of these clarifier diameters was based on balancing surface area and OFR, while maintaining compact design feasibility in a pilot-scale system. The transition from the 1.0 m to the 1.4 m diameter clarifier aimed to evaluate the effect of increased settling surface area on SS removal efficiency and effluent quality. It is essential to distinguish between the overall SS removal efficiency of the system and the separation performance in the clarifiers. Both clarifiers achieved a 97 $\pm$ 2 % MLSS removal, which indicates strong solids separation efficiency. The SS removal efficiency in the HRAS pilot plant had an average value of 76 %, similar to the 70 % reported by [57], higher than the 50 % reported by [58] and at the same level that PC (50–70 %) [39].

Despite the wide variation in the influent SS values (average 401 $\pm$ 176 mg L^{-1}), effluent SS values showed less dispersion. Over the operation period from days 100–350, the 1.0 m diameter clarifier presented an effluent SS of 103 $\pm$ 43 mg L^{-1}, while the 1.4 m diameter clarifier improved upon this, with an average of 57 $\pm$ 26 mg L^{-1}. Overall, the HRAS process acted as a filter for influent SS peak loads, buffering these loads for subsequent activated sludge processes.

The maximum and average SS removal values recorded were 1050 mg L^{-1} and 315 $\pm$ 175 mg L^{-1}, respectively. These values demonstrate the long-term stability of the HRAS process in handling varying SS loads and the efficient removal of SS over extended

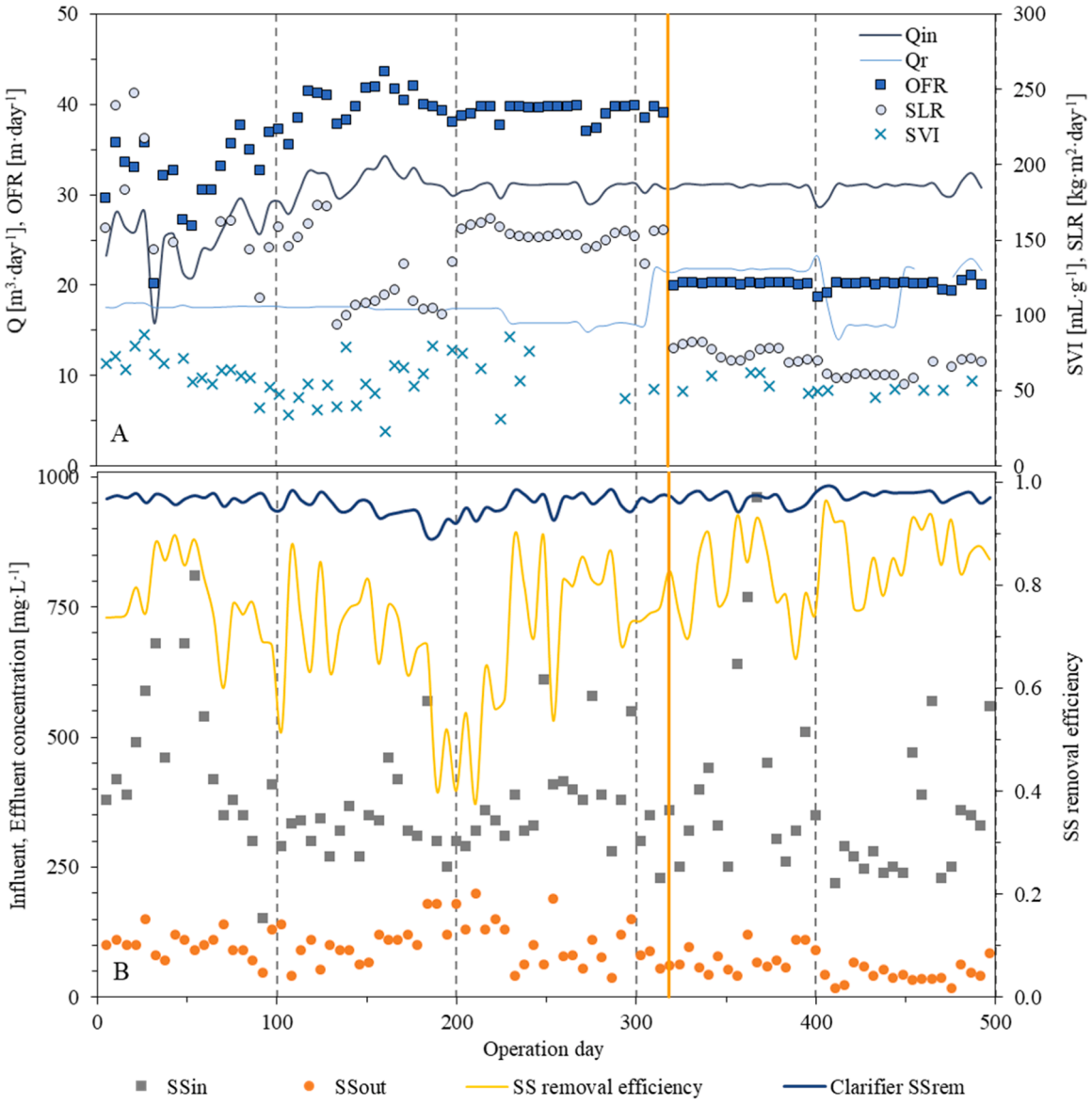

Fig. 5. Daily monitoring of A) influent and recirculation flowrate, OFR, SLR and SVI; and B) SS concentrations at the influent and effluent, and SS removal efficiency. Solid vertical line denotes the change of the clarifier under operation.

operational periods.

The relationship between overall SS removal and influent SS concentration (Fig. 6) revealed a near-unity slope, indicating the presence of non-settling SS regardless of influent characteristics. This finding aligns with Parker [36] bimodal particle size distribution, which distinguishes between two particle types: larger particles that dominate sedimentation processes due to their high settling velocities, and smaller particles (0.5–5 μm) that originate from dispersed bacterial growth, or the erosion of larger particles caused by turbulence between the biological reactor and the settling tank. These smaller particles exhibit low settling velocities, making them non-settleable and prone to remain in the effluent unless removed through additional processes such as coagulation or advanced clarification. This supports the importance of considering SS fractionation – such as inorganic settleable solids (ISS), unbiodegradable particulates organics (UOP), biodegradable particulates organics (BPO), and the particle size distribution - in future clarifier optimization studies for HRAS.

The use of two clarifiers allowed the assessment of operational parameters. The 1.0 m diameter clarifier used until day 350 operated at an OFR (Eq. 1) of approximately 1.6 m h^{-1}, aligning with PC standards (1.2–2.0 m h^{-1}). This clarifier achieved effluent SS concentrations between 91 and 119 mg L^{-1}, comparable to PCs (typically 90–120 mg L^{-1}). In contrast, the 1.4 m diameter clarifier, used from day 351 onwards, was operated at an OFR of 0.8 m h^{-1}, similar to SCs in CAS systems (0.66–1.6 m h^{-1}). The larger diameter clarifier achieved superior performance, with effluent SS concentrations of 44–69 mg L^{-1}, although still higher than those typically observed in SCs (20–30 mg L^{-1}).

Notably, the significant improvement in SS removal efficiency from 70 % to 85 % upon reducing the OFR highlights the beneficial impact of low OFR values. Lowering OFR improved SS removal efficiency, emphasizing the necessity of controlling OFR to achieve optimal removal of discrete and flocculent settling [59].

The SLR (Eq. 2) was also related to the clarifier surface area, presenting an average of 147 kg m^{-2} day^{-1} and 71 kg m^{-2} day^{-1} for the first and second clarifiers, as depicted in Fig. 5A. Although the SLR did not limit the SS removal efficiency, enlarging the clarifier surface ensured the system's stability while slightly improving the SVI_{30} (Fig. 5A). However, for the range of SVI_{30} during the whole operational period, 30–80 mL g^{-1}, no relation was found with the SS removal

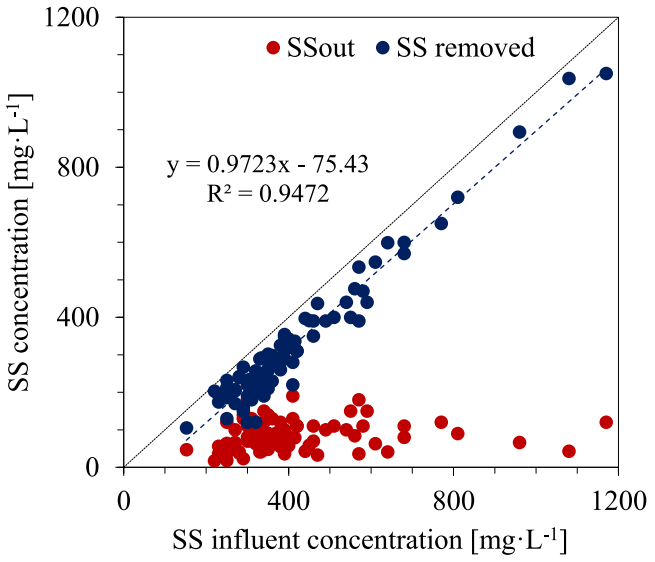

Fig. 6. Relation between influent and effluent and removed suspended solids.

efficiency (see Fig. S8).

3.5. Clarifiers performance analysis

3.5.1. Sludge stratification

A detailed stratification study was conducted to examine the distribution of suspended solids within the clarifier, identifying zones with distinct SS concentrations and biomass inventory. Fig. 7 shows the SS concentrations in the clarifier according to the five sampling points at different heights (shown in Fig. S2). The upper clarification zone, between the sludge inlet and water outlet level, plays a critical role in capturing and removing particles that settle slowly. Here, SS concentration decreases from 600 mg L^{-1} to 100 mg L^{-1} moving upwards. Below, in the sludge settling zone, where the clarifier stretches from the sludge inlet level down to the beginning of the conical section, the SS concentration stabilizes around 700 mg L^{-1}. At the base of the clarifier is the sludge compaction zone, where the solids are concentrated before being removed with the maximum SS concentration of 5000 mg L^{-1}.

Additionally, Fig. 7 illustrates biomass distribution within the clarifier, showing 38 % of the total MLSS inventory in the compaction zone, 28 % below the influent point, 22 % above the influent point, and 12 % in the clarification zone. The observed stratification supports stable effluent quality by ensuring effective biomass retention while preventing excessive SS carryover. The total biomass inventory within the clarifier was quantified at 1.8 kg MLSS, compared to 1.85 kg MLSS in the reactor (0.8 m^3 volume, Fig. 1A). This near-equal distribution between the reactor and clarifier highlights the critical role of the clarifier in biomass retention, aligning with the findings of [28], who reported a 60–40 % split between clarifier and reactor biomass.

These results contrast with conventional CAS systems, where 85–90 % of the biomass is typically retained within the reactor [48]. The balanced distribution observed in the HRAS process reinforces its capacity to efficiently handle solids while maintaining a stable effluent SS concentration, confirming that the stratification strategy, controlled by the recirculation flow, is already optimal for process stability.

However, the HRAS system generates waste sludge with a lower concentration (<0.6 %) compared to conventional primary clarifiers (1 %), requiring more robust thickening equipment. Increasing sludge concentration by elevating the sludge blanket height or altering wasting intervals poses a risk of re-dissolving stored carbon within cells, as [31] highlighted. This underscores the importance of careful operational management to prevent compromising sludge quality and efficiency.

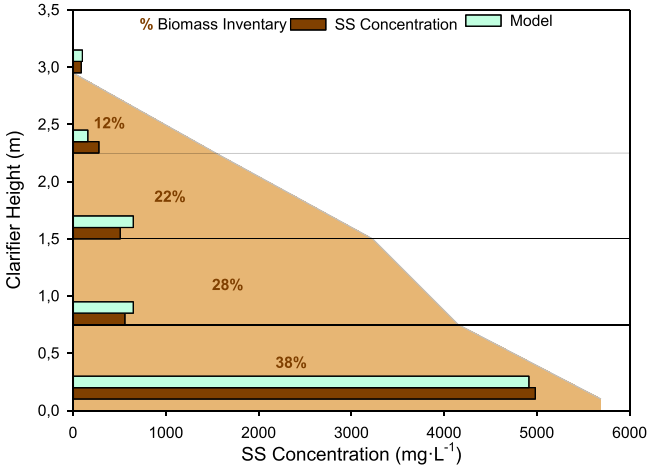

Fig. 7. Suspended solids (SS) concentration at different heights of the clarifier and sludge distribution calculated by Equations S1–S5. The yellow area represents the percentage of biomass retained at each height, ranging from 0 % at the top to 38 % at the bottom.

3.5.2. Zone settling velocity

Batch settling tests were conducted on sludge samples at different initial MLSS concentrations to assess the settling behaviour over time and determine the ZSV (Fig. S9). As shown in Fig. 8, at an MLSS concentration of 2000 mg L^{-1}, the ZSV was 5.1 m h^{-1}, decreasing to 4.12 m h^{-1} at 2500 mg L^{-1}. This 19 % reduction in ZSV with increasing MLSS concentration highlights the significant impact of MLSS concentration on the settling efficiency.

For comparison, the ZSV values reported in the CAS process study [42] - 3.3 and 2.1 m h^{-1} at the same MLSS concentrations - are also plotted in Fig. 8. These data highlight the superior settleability of HRAS sludge, as the impact of increasing MLSS on ZSV is less pronounced in HRAS systems.

Further analysis using the Vesilind model allowed a deeper exploration of the dynamics between MLSS concentration, ZSV, and clarifier performance. The calibration of the model against the experimental ZSV data (Fig. 8) resulted in crucial parameters (Eq. 12) of V_o = 12.02 m h^{-1} and r_h = 0.428 m^3 kg^{-1} . The comparative analysis of SS clarifier stratification between the five sampling points in the pilot plant and the sludge stratification model (Equations S1-S5) is provided in Fig. 7,

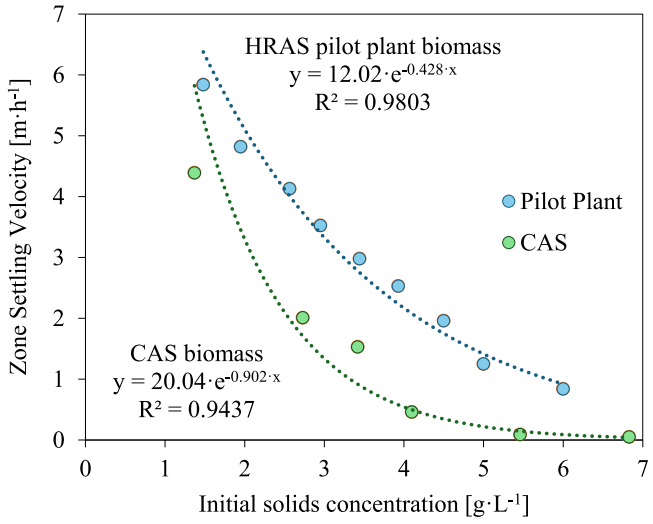

Fig. 8. Zone settling velocity (ZSV) as a function of the initial sludge concentration (MLSS) for HRAS pilot plant biomass (blue dots) compared with values reported by Torfs et al. (2016) for CAS biomass (green dots).

which underscores the accuracy of the simulation, demonstrating good alignment between the observed data and the model predictions.

3.5.3. Solids flux analysis

The solids flux analysis was conducted using Eqs. 13–16, comparing the two clarifiers used in this study. Resulting from the bulk and gravity flux, the total solids flux diagram for the pilot plant clarifier is depicted in Fig. 9. The solids flux of the narrower clarifier is faster due to the quicker SFu, with a maximum SFt occurring at a solids concentration of 3 g L^{-1}. In turn, the flux of the 1.4 m diameter clarifiers is more influenced by the SFg than the bulk movement, with a maximum flux at a solids concentration of 2.6 g L^{-1}, which is closer to the operating MLSS concentration, highlighting the importance of MLSS concentration in sludge settleability and management.

The analysis reveals that the limiting solids flux for each clarifier is 140 kg m^{-2} day^{-1} for the 1.4 m diameter clarifier and 250 kg m^{-2} day^{-1} for the 1.0 m diameter clarifier. In both cases, the solid loading was lower than the limiting flux, as shown in Fig. 5A (SLR). This indicates that the clarifiers operate below their maximum load management capacity, so the OFR becomes a more critical design and operational parameter. Thus, the system's performance was not constrained by the solids flux, which could handle higher solid concentration, but rather by the hydraulic loading rate. Therefore, optimizing the OFR would have a more significant impact than focusing solely on solids loading, ensuring effective separation while preventing hydraulic overloading.

Alternative technologies, such as lamella clarifiers, could further enhance solids separation efficiency, particularly for discrete flocculent particles in the upper section. These systems increase the effective settling surface area, improving fine particle removal and overall clarifier performance [60,61].

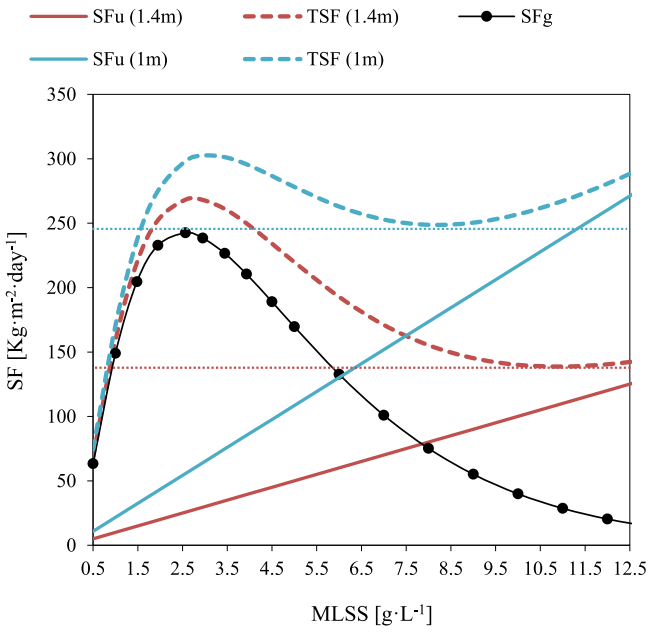

Fig. 9. Solids flux and solids concentration diagram for the two clarifiers studied (1.0-m diameter in blue, 1.4-m diameter in red). SFg: solid flux due to gravity; SFu: solid flux resulting from bulk movement; SFt: total solid mass flux. The limiting flux for each clarifier is indicated in dotted lines.

4. Conclusions

This study thoroughly evaluates the HRAS process, highlighting its performance optimization and long-term stability over nearly 500 days of continuous operation. The key conclusions drawn from this research are as follows:

- Adjusting the MLSS set point between 1800 and 2100 mg L^{-1} proved essential for maintaining settling stability while dynamically responding to variations in influent characteristics. The consistent SRT of 0.2 ± 0.05 days demonstrated the process's efficiency-enhancing COD harvesting (58 %).
- Despite operating under elevated organic loading conditions of 10.5 ± 3.5 kg_{COD} kg_{MLSS}^{-1} d^{-1}, the HRAS pilot plant maintained an average ORR of 58 %, highlighting the system's ability to handle fluctuating influent loads effectively.
- The pilot plant successfully managed the oxygen supply according to demand. The SOC metrics indicated that the oxygen demand varied significantly with operational conditions and influent characteristics, reinforcing the need for precise sCOD monitoring to minimize COD oxidation.
- The low SER indicated rapid biomass turnover, emphasizing the influence of influent solids on biomass dynamics. However, the results showed that the HRAS system can maintain sustained biological activity without requiring a PC. The absence of sludge bulking, even at low DO levels, and the diverse microbial community observed challenge the notion that such diversity is exclusive to conventional systems. Additionally, the average SVI_{30} value of 55 mL g^{-1} demonstrated superior settling characteristics compared to traditional activated sludge processes.
- The evaluation of SS removal demonstrated high efficiency in buffering SS influent peaks. Using a 1 m diameter clarifier, the influent SS removal efficiency averaged 71 % at an OFR of 1.6 m h^{-1}, while enlarging the clarifier to 1.4 m in diameter resulted in a consistent efficiency of 85 % at an OFR of 0.8 m h^{-1}. Thus, an appropriate clarifier design appears critical to efficient and stable operation.
- The biomass stratification analysis demonstrated that the clarifier retained a substantial fraction of MLSS, reinforcing its essential role in maintaining process stability and effluent quality.
- The solids flux analysis confirmed that the clarifiers were operating below their limiting solids flux, suggesting that the system was not constrained by solids loading but rather by hydraulic loading. Future studies should focus on optimizing OFR to improve HRAS clarifier performance further, particularly under high SS influent conditions.

CRediT authorship contribution statement

Hèctor Monclús: Writing – review & editing, Supervision, Funding acquisition. **Sara García:** Resources, Project administration. **Juan M. Lema:** Writing – review & editing, Validation. **Oriol Carbó:** Investigation, Data curation. **Andrea Turolla:** Writing – review & editing, Validation. **Joan Canals:** Writing – original draft, Methodology, Conceptualization. **Alba Cabrera-Codony:** Writing – original draft, Visualization, Formal analysis.

Declaration of Competing Interest

The authors declare that they have no known competing financial interests or personal relationships that could have appeared to influence the work reported in this paper.

Acknowledgements

GS Inima Environment would like to thank the Consorci Bess- Tordera for allowing the pilot plant installation in the Montornès WWTP and for their full collaboration during its operation, especially with the WWTP operating staff. We acknowledge the Centre for the Development of Industrial Technology (CDTI) Spanish Ministry of Science, Innovation and Universities (MCIU) for funding this research. Hèctor Monclús and Alba Cabrera-Codony acknowledge Agencia Estatal de Investigación of the MCIU for partially funding this research through the Ramon y Cajal Research Fellowship (RYC2019-026434-I) and Juan de la Cierva

Fellowship (IJC2019-038874-I). LEQUIA has been recognised as a "consolidated research group" (Ref 2021 SGR1352) by the Catalan Ministry of Research and Universities.

Appendix A. Supporting information

Supplementary data associated with this article can be found in the online version at doi:10.1016/j.jece.2025.116165.

Data availability

Data will be made available on request.

References

[1] A. Rahman, H. De Clippeleir, W. Thomas, J.A. Jimenez, B. Wett, A. Al-Omari, S. Murthy, R. Riffat, C. Bott, A-stage and high-rate contact-stabilization performance comparison for carbon and nutrient redirection from high-strength municipal wastewater, Chem. Eng. J. 357 (2019) 737–749, https://doi.org/10.1016/J.CEJ.2018.09.206.

[2] Z. Wu, Z. Zhu, X. Zhang, L. Zhou, K. Zhang, P. Wu, New insights into carbon capture and re-direction technologies for wastewater resource recovery: a critical review, J. Water Process Eng. 59 (2024) 105105, https://doi.org/10.1016/j.jwpe.2024.105105.

[3] R.-S.S. Guthi, K. Tondera, S. Gillot, P. Buffière, M. Boillot, F. Chazarenc, A-Stage process – challenges and drawbacks from lab to full scale studies: a review, Water Res. 226 (2022) 119044, https://doi.org/10.1016/j.watres.2022.119044.

[4] A. AlSayed, M. Soliman, A. Eldyasti, The A-stage process to promote bioflocculation and microbial storage for carbon redirection: current perspectives and future research directions, Rev. Environ. Sci. Biotechnol. 22 (2023) 1009–1035, https://doi.org/10.1007/s11157-023-09673-0.

[5] H. Gulhan, R.F. Dizaji, M.N. Hamidi, A.M. Abdelrahman, S. Basa, S. Cingoz, I. Koyuncu, H. Guven, H. Ozgun, M.E. Ersahin, R.K. Dereli, I. Ozturk, Modelling of high-rate activated sludge process: assessment of model parameters by sensitivity and uncertainty analyses, Sci. Total Environ. 915 (2024) 170102, https://doi.org/10.1016/j.scitotenv.2024.170102.

[6] A. Rahman, E. Shen, B. Wett, P. Aichinger, T. Constantine, Stories of biologically enhanced carbon diversion technology in the age of biological nutrient removal process – Origin, evolution and milestones, J. Water Process Eng. 70 (2025) 106971, https://doi.org/10.1016/j.jwpe.2025.106971.

[7] V. Tirkey, E.M. Goonesekera, A. Kovalovszki, B.F. Smets, A. Dechesne, B. Valverde-Pérez, Short sludge age denitrification as alternative process for energy and nutrient recovery, Bioresour. Technol. 366 (2022) 128184, https://doi.org/10.1016/j.biortech.2022.128184.

[8] Y. Li, C. Wang, R. Feng, J. Huang, Y. Wang, H. Li, Sustainability transformation of coal chemical wastewater treatment through carbon capture processes, J. Environ. Chem. Eng. 13 (2025) 115083, https://doi.org/10.1016/j.jece.2024.115083.

[9] J. Canals, A. Cabrera-Codony, O. Carbó, J. Torán, M. Martín, M. Baldi, B. Gutiérrez, M. Poch, A. Ordóñez, H. Monclús, High-rate activated sludge at very short SRT: key factors for process stability and performance of COD fractions removal, Water Res. 231 (2023), https://doi.org/10.1016/j.watres.2023.119610.

[10] N. Rey-Martínez, A. Barreiro-López, A. Guisasola, J.A. Baeza, Comparing continuous and batch operation for high-rate treatment of urban wastewater, Biomass Bioenergy 149 (2021) 106077.

[11] R. Gori, L.M. Jiang, R. Sobhani, D. Rosso, Effects of soluble and particulate substrate on the carbon and energy footprint of wastewater treatment processes, Water Res. 45 (2011) 5858–5872, https://doi.org/10.1016/j.watres.2011.08.036.

[12] M. Jia, K. Solon, D. Vandeplassche, H. Venugopal, E.I.P. Volcke, Model-based evaluation of an integrated high-rate activated sludge and mainstream anammox system, Chem. Eng. J. 382 (2020) 122878, https://doi.org/10.1016/J.CEJ.2019.122878.

[13] J. Carrera, O. Carbó, S. Doñate, M.E. Suárez-Ojeda, J. Pérez, Increasing the energy production in an urban wastewater treatment plant using a high-rate activated sludge: pilot plant demonstration and energy balance, J. Clean. Prod. 354 (2022) 131734, https://doi.org/10.1016/j.jclepro.2022.131734.

[14] S. Haider, K. Svardal, P.A. Vanrolleghem, H. Kroiss, The effect of low sludge age on wastewater fractionation (SS, SI), Water Sci. Technol. 47 (2003) 203–209, https://doi.org/10.2166/wst.2003.0606.

[15] B. Wett, K. Buchauer, C. Fimml, Energy self-sufficiency as a feasible concept for wastewater treatment systems, in: IWA Leading Edge Technology Conference, Singapure, 2007: pp. 21–24.

[16] J. Jimenez, M. Miller, C. Bott, S. Murthy, H. De Clippeleir, B. Wett, High-rate activated sludge system for carbon management - evaluation of crucial process mechanisms and design parameters, Water Res. 87 (2015) 476–482, https://doi.org/10.1016/j.watres.2015.07.032.

[17] J. Canals, A. Cabrera-Codony, O. Carbó, M. Baldi, B. Gutiérrez, A. Ordoñez, M.J.M. J. Martín, M. Poch, H. Monclús, Nutrients removal by high-rate activated sludge and its effects on the mainstream wastewater treatment, Chem. Eng. J. 479 (2024) 147871, https://doi.org/10.1016/j.cej.2023.147871.

[18] B. Böhnke, B. Diering, S. Zuckut, Cost-effective wastewater treatment process for removal of organics and nutrients - ScienceBase-Catalog, Water Eng. Manag. 144 (1997) 18–21.

[19] M. Miller, M. Elliott, M. Kinyua, … B.W.-… H.-R.A., U. 2015, Optimizing High-Rate Activated Sludge:Organic Substrate for Biological Nitrogen Removal and Energy Recovery, Vtechworks.Lib.Vt.Edu, 2015. ⟨https://vtechworks.lib.vt.edu/bitstream/handle/10919/78208/Miller_MW_D_2015.pdf?sequence= 1&isAllowed=y#page= 95⟩ (Accessed 31 August 2023).

[20] S.J. Christian, S.R. Grant, K.S. Singh, R.C. Landine, Performance of a high-rate/high-shear activated sludge bioreactor treating biodegradable wastewater, Environ. Technol. 29 (2008) 837–846, https://doi.org/10.1080/09593330801987616.

[21] I. Sancho, S. Lopez-Palau, N. Arespacochaga, J.L.L. Cortina, New concepts on carbon redirection in wastewater treatment plants: a review, Sci. Total Environ. 647 (2019) 1373–1384, https://doi.org/10.1016/J.SCITOTENV.2018.08.070.

[22] C. Zhang, A. Guisasola, J.A. Baeza, Achieving simultaneous biological COD and phosphorus removal in a continuous anaerobic/aerobic A-stage system, Water Res. 190 (2021) 116703, https://doi.org/10.1016/j.watres.2020.116703.

[23] P. Regmi, M.W. Miller, B. Holgate, R. Bunce, H. Park, K. Chandran, B. Wett, S. Murthy, C.B. Bott, Control of aeration, aerobic SRT and COD input for mainstream nitritation/denitritation, Water Res. 57 (2014) 162–171, https://doi.org/10.1016/J.WATRES.2014.03.035.

[24] D. Bolzonella, P. Pavan, P. Battistoni, F. Cecchi, Mesophilic anaerobic digestion of waste activated sludge: Influence of the solid retention time in the wastewater treatment process, Process Biochem. 40 (2005) 1453–1460, https://doi.org/10.1016/J.PROCBIO.2004.06.036.

[25] A. AlSayed, M. Soliman, A. ElDyasti, Mechanistic assessment reveals the significance of HRT and MLSS concentration in balancing carbon diversion and removal in the A-stage process, J. Environ. Manag. 334 (2023), https://doi.org/10.1016/j.jenvman.2023.117527.

[26] Y. Wei, W. Xia, M. Ye, F. Chen, Y. Qian, Y.-Y. Li, Optimizing hydraulic retention time of high-rate activated sludge designed for potential integration with partial nitritation/anammox in municipal wastewater treatment, Bioresour. Technol. 401 (2024) 130710, https://doi.org/10.1016/j.biortech.2024.130710.

[27] T. Nogaj, A. Randall, J. Jimenez, I. Takacs, C. Bott, M. Miller, S. Murthy, B. Wett, Modeling of organic substrate transformation in the high-rate activated sludge process, Water Sci. Technol. 71 (2015) 971–979, https://doi.org/10.2166/wst.2015.051.

[28] H. Hauduc, A. Al-Omari, B. Wett, J. Jimenez, H. De Clippeleir, A. Rahman, T. Wadhawan, I. Takacs, Colloids, flocculation and carbon capture – a comprehensive plant-wide model, Water Sci. Technol. 79 (2019) 15–25, https://doi.org/10.2166/WST.2018.454.

[29] W. Zhao, Y.P. Ting, J.P. Chen, C.H. Xing, S.Q. Shi, Advanced primary treatment of waste water using a bio-flocculation-adsorption sedimentation process, Acta Biotechnol. 20 (2000) 53–64, https://doi.org/10.1002/abio.370200109.

[30] M. Jetten, S. Hom, M. Van Loosdrecht, Towards a more sustainable municipal wastewater treatment system, Water Sci. Technol. 35 (1997), https://doi.org/10.1016/S0273-1223(97)00195-9.

[31] D. Rosso, A. Al-Omari, M. Garrido-Baserba, H. de Clippeleir, Carbon Capture and Management Strategies for Energy Harvest from Wastewater, The Water Research Foundation, 2019. ⟨https://www.waterrf.org/research/projects/carbon-capture-and-management-strategies-energy-harvest-wastewater⟩ (Accessed 6 August 2022).

[32] M.S. De Graaff, T. Van Den Brant, K. Roest, T.P.H. Van Den Brand, K. Roest, M.H. Zandvoort, O. Duin, M.C.M. Van Loosdrecht, T. Van Den Brant, K. Roest, Full-Scale Highly-Loaded Wastewater Treatment Processes (A-Stage) to Increase Energy Production from Wastewater: Performance and Design Guidelines, Https://Home.Liebertpub.Com/Ees 33 (2016) 571–577. ⟨https://doi.org/10.1089/EES.2016.0022⟩.

[33] W.A.S.K. Mancell-Egala, D.J. Kinnear, K.L. Jones, H. De Clippeleir, I. Takács, S. N. Murthy, Limit of stokesian settling concentration characterizes sludge settling velocity, Water Res 90 (2016) 100–110, https://doi.org/10.1016/j.watres.2015.12.007.

[34] Z. Yuan, G. Olsson, R. Cardell-Oliver, K. van Schagen, A. Marchi, A. Deletic, C. Urich, W. Rauch, Y. Liu, G. Jiang, Sweating the assets – The role of instrumentation, control and automation in urban water systems, Water Res. 155 (2019) 381–402, https://doi.org/10.1016/j.watres.2019.02.034.

[35] G. Ekama, G. Ekama, J. Barnard, I.A.O.W. Quality, F. Gunthert, P. Krebs, J. Mccorquodale, D. Parker, E. Wahlberg, Secondary settling tanks: theory, modelling, design and operation, IAWQ London, U.K, 1997.

[36] D.S. Parker, W.J. Kaufman, D. Jenkins, Physical conditioning of activated sludge floc, J. Water Pollut. Control Fed. 43 (9) (1971) 1817–1833. ⟨https://www.jstor.org/stable/25037177?casa_token=ExrzKosrjRYAAAAA%3AnGrlm1y-PcT0m95eZVwnqZMWqq8eIQC-XmihKUuCGW2PG9wwvt6jQt69QkK_8US1-jwoEMDinz7Gfe-Kisi3IvbuaCg0phpZg3PXt4T100A3HjUKbX9kPg⟩ (accessed December 18, 2024).

[37] J.A. Jimenez, E.J. La Motta, D.S. Parker, Kinetics of removal of particulate chemical oxygen demand in the activated-sludge process, Water Environ. Res. 77 (2005) 437–446, https://doi.org/10.2175/106143005X67340.

[38] G.A. Ekama, M.C. Wentzel, S.W. Sötemann, Tracking the inorganic suspended solids through biological treatment units of wastewater treatment plants, Water Res. 40 (2006) 3587–3595, https://doi.org/10.1016/j.watres.2006.05.034.

[39] Eddy Metcalf. Wastewater Engineering, 4th Ed., McGraw-Hill, New York, 2003.

[40] P. Dold, M. Fairlamb, Estimating oxygen transfer KLa, sote and air flow requirements in fine bubble diffused air systems, Proc. Water Environ. Fed. 2001 (2012) 780–791, https://doi.org/10.2175/193864701790864070.

[41] M. Schwarz, J. Behnisch, J. Trippel, M. Engelhart, M. Wagner, Oxygen transfer in two-stage activated sludge wastewater treatment plants, Water 13 (2021) 1964, https://doi.org/10.3390/w13141964.

[42] E. Torfs, S. Balemans, F. Locatelli, S. Diehl, R. Bürger, J. Laurent, P. François, I. Nopens, On constitutive functions for hindered settling velocity in 1-D settler models: Selection of appropriate model structure, 2016. ⟨https://doi.org/10.1016/j.watres.2016.11.067⟩.
[43] P.A. Vesilind, Theoretical considerations: design of prototype thickeners from batch settling tests, Water Sew. Works 115 (1968) 302–307.
[44] I. Takacs, G.G. Patry, D. Nolasco, A dynamic model of the clarification-thickening process, Water Res. 25 (1991) 1263–1271, https://doi.org/10.1016/0043-1354(91)90066-Y.
[45] A.L. Amaral, D.P. Mesquita, E.C. Ferreira, Automatic identification of activated sludge disturbances and assessment of operational parameters, Chemosphere 91 (2013) 705–710, https://doi.org/10.1016/J.CHEMOSPHERE.2012.12.066.
[46] D. Das, T.M. Keinath, D.S. Parker, E.J. Wahlberg, Floc breakup in activited sludge plants, Water Environ. Res. 65 (1993) 138–145, https://doi.org/10.2175/WER.65.2.6.
[47] V. Diamantis, W. Verstraete, A. Eftaxias, B. Bundervoet, S.E. Vlaeminck, P. Melidis, A. Aivasidis, Sewage pre-concentration for maximum recovery and reuse at decentralized level, Water Sci. Technol. 67 (2013) 1188–1193, https://doi.org/10.2166/WST.2013.639.
[48] R.W. Crites, G. Tchobanoglous, Small and Decentralized Wastewater Management Systems, WCB/McGraw-Hill, 1998. ⟨http://books.google.com/books?id=yx9SAAAAMAAJ&pgis=1⟩.
[49] B. Wett, P. Aichinger, M. Hell, M. Andersen, L. Wellym, Y. Fukuzaki, Y.S. Cao, G. Tao, J. Jimenez, I. Takacs, C. Bott, S. Murthy, Operational and structural A-stage improvements for high-rate carbon removal, Water Environ. Res. 92 (2020) 1983–1989, https://doi.org/10.1002/wer.1354.
[50] A. Taboada-Santos, E. Rivadulla, L. Paredes, M. Carballa, J. Romalde, J.M. Lema, Comprehensive comparison of chemically enhanced primary treatment and high-rate activated sludge in novel wastewater treatment plant configurations, Water Res. 169 (2020) 115258, https://doi.org/10.1016/j.watres.2019.115258.
[51] Y. Jo, J. Park, G.-B. Kim, Y. Lee, S.-H. Kim, Carbon redirection pathway, energy recovery potential, and microbial population dynamics in high-rate activated sludge, J. Water Process Eng. 64 (2024) 105682, https://doi.org/10.1016/j.jwpe.2024.105682.
[52] A. Rahman, M. Hasan, F. Meerburg, J.A. Jimenez, M.W. Miller, C.B. Bott, A. Al-Omari, S. Murthy, A. Shaw, H. De Clippeleir, R. Riffat, Moving forward with A-stage and high-rate contact-stabilization for energy efficient water resource recovery facility: mechanisms, factors, practical approach, and guidelines, J. Water Process Eng. 36 (2020), https://doi.org/10.1016/j.jwpe.2020.101329.
[53] A. Rahman, F. Meerburg, S. Ravadagundhi, B. Wett, J. Jimenez, C. Bott, A. Al-Omari, R. Riffat, S. Murthy, H. De Clippeleir, Bioflocculation management through high-rate contact-stabilization: a promising technology to recover organic carbon from low-strength wastewater, Water Res. 104 (2016) 485–496, https://doi.org/10.1016/j.watres.2016.08.047.
[54] F.A. Meerburg, N. Boon, T. Van Winckel, J.A.R. Vercamer, I. Nopens, S. E. Vlaeminck, Toward energy-neutral wastewater treatment: a high-rate contact stabilization process to maximally recover sewage organics, Bioresour. Technol. 179 (2015) 373–381.
[55] O. Carbó, J. Teixidó, J. Canals, A. Ordóñez, A. Magrí, M. Baldi, B. Gutiérrez, J. Colprim, Achieving mainstream partial nitritation with aerobic granular sludge treating high-rate activated sludge effluent, J. Water Process Eng. 60 (2024) 105165, https://doi.org/10.1016/j.jwpe.2024.105165.
[56] W.A.S.K. Mancell-Egala, C. Su, I. Takacs, J.T. Novak, D.J. Kinnear, S.N. Murthy, H. De Clippeleir, Settling regimen transitions quantify solid separation limitations through correlation with floc size and shape, Water Res. 109 (2017) 54–68, https://doi.org/10.1016/j.watres.2016.10.080.
[57] M. Miller, M. Elliott, M. Kinyua, … B.W.-… H.-R.A., U. 2015, Optimizing High-Rate Activated Sludge:Organic Substrate for Biological Nitrogen Removal and Energy Recovery, Vtechworks.Lib.Vt.Edu, 2015.
[58] M.S. De Graaff, T. Van Den Brant, K. Roest, T.P.H. Van Den Brand, K. Roest, M.H. Zandvoort, O. Duin, M.C.M. Van Loosdrecht, T. Van Den Brant, K. Roest, Full-Scale Highly-Loaded Wastewater Treatment Processes (A-Stage) to Increase Energy Production from Wastewater: Performance and Design Guidelines, Https://Home.Liebertpub.Com/Ees 33 (2016) 571–577. ⟨https://doi.org/10.1089/EES.2016.0022⟩.
[59] T. Van Winckel, X. Liu, S.E. Vlaeminck, I. Takács, A. Al-Omari, B. Sturm, B. V. Kjellerup, S.N. Murthy, H. De Clippeleir, Overcoming floc formation limitations in high-rate activated sludge systems, Chemosphere 215 (2019) 342–352, https://doi.org/10.1016/J.CHEMOSPHERE.2018.09.169.
[60] H. Zhang, S. Zheng, X. Zhang, S. Duan, S. Li, Optimizing the inclined plate settler for a high-rate microaerobic activated sludge process for domestic wastewater treatment: a theoretical model and experimental validation, Int. Biodeterior. Biodegrad. 154 (2020) 105060, https://doi.org/10.1016/j.ibiod.2020.105060.
[61] H. Gulhan, M.N. Hamidi, A.M. Abdelrahman, M. Fakioglu, B. Mese, M. Yoruk, E. S. Kurt, I. Koyuncu, H. Guven, H. Ozgun, M.E. Ersahin, I. Ozturk, Long term experiences in a pilot-scale high-rate activated sludge system with lamella clarifier: effluent quality and carbon capture, J. Water Process Eng. 49 (2022) 103138, https://doi.org/10.1016/j.jwpe.2022.103138.